0026-895X/11/8001-1–13$25.00
MOLECULAR PHARMACOLOGY
Copyright © 2011 The American Society for Pharmacology and Experimental Therapeutics
Mol Pharmacol 80:1–13, 2011

Vol. 80, No. 1
70540/3693644
Printed in U.S.A.

A Novel Family of Insect-Selective Peptide Neurotoxins Targeting Insect Large-Conductance Calcium-Activated K^+ Channels Isolated from the Venom of the Theraphosid Spider *Eucratoscelus constrictus*

Monique J. Windley, Pierre Escoubas,[1] Stella M. Valenzuela, and Graham M. Nicholson

Neurotoxin Research Group, School of Medical & Molecular Biosciences, University of Technology, Sydney, Australia (M.J.W., S.M.V., G.M.N.); and Université de Nice Sophia Antipolis, Institut de Pharmacologie Moléculaire et Cellulaire, Centre National de la Recherche Scientifique, Valbonne, France (P.E.)

Received December 14, 2010; accepted March 14, 2011

ABSTRACT

Spider venoms are actively being investigated as sources of novel insecticidal agents for biopesticide engineering. After screening 37 theraphosid spider venoms, a family of three new "short-loop" inhibitory cystine knot insecticidal toxins (κ-TRTX-Ec2a, κ-TRTX-Ec2b, and κ-TRTX-Ec2c) were isolated and characterized from the venom of the African tarantula *Eucratoscelus constrictus*. Whole-cell patch-clamp recordings from cockroach dorsal unpaired median neurons revealed that, despite significant sequence homology with other theraphosid toxins, these 29-residue peptides lacked activity on insect voltage-activated sodium and calcium channels. It is noteworthy that κ-TRTX-Ec2 toxins were all found to be high-affinity blockers of insect large-conductance calcium-activated K^+ (BK_{Ca}) channel currents with IC_{50} values of 3 to 25 nM. In addition, κ-TRTX-Ec2a caused the inhibition of insect delayed-rectifier K^+ currents, but only at significantly higher concentrations. κ-TRTX-Ec2a and κ-TRTX-Ec2b demonstrated insect-selective effects, whereas the homologous κ-TRTX-Ec2c also resulted in neurotoxic signs in mice when injected intracerebroventricularly. Unlike other theraphosid toxins, κ-TRTX-Ec2 toxins induce a voltage-independent channel block, and therefore, we propose that these toxins interact with the turret and/or loop region of the external entrance to the channel and do not project deeply into the pore of the channel. Furthermore, κ-TRTX-Ec2a and κ-TRTX-Ec2b differ from other theraphotoxins at the C terminus and positions 5 to 6, suggesting that these regions of the peptide contribute to the phyla selectivity and are involved in targeting BK_{Ca} channels. This study therefore establishes these toxins as tools for studying the role of BK_{Ca} channels in insects and lead compounds for the development of novel insecticides.

Introduction

Conventional agrochemicals are used currently to combat phytophagous pest insects and vectors of human and livestock diseases. In addition to the issue that many have been deregistered because of human health risks and environmental concerns, one of the major dilemmas associated with these agents is the increasing development of insecticide resistance (Nicholson, 2007a). Unfortunately, wide use and the limited target range of these compounds have resulted in an increasing incidence of insecticide resistance and a lack of effective insecticide control. Therefore, there is now a push to pursue novel insect-selective compounds with alternate targets as leads for new insecticidal agents (Nicholson, 2007b; King et al., 2008a). The validation of a novel insecticidal target and

This work was supported in part by the Australian Research Council [Grant DP0559396]; the Department of Education, Science and Training [Grant FR050106]; the Centre National de la Recherche Scientifique–Projet International de Coopération Scientifique [Grant 3603]; and an Australian Postgraduate Award.

[1] Current affiliation: VenomeTech, Valbonne, France.

Article, publication date, and citation information can be found at http://molpharm.aspetjournals.org.
doi:10.1124/mol.110.070540.

ABBREVIATIONS: Na_V channel, voltage-activated sodium channel; 4-AP, 4-aminopyridine; BK_{Ca} channel, large-conductance Ca^{2+} and voltage-activated K^+ channel ($K_{Ca}1.1$, Maxi-K, BK, Slo1); Ca_V channel, voltage-activated Ca^{2+} channel; ChTx, charybdotoxin (potassium channel scorpion toxin 1.1); DUM, dorsal unpaired median; HVA, high-voltage-activated; HXTX, hexatoxin (from the venom of spiders belonging to the family Hexathelidae); IK_{Ca}, intermediate-conductance Ca^{2+}-activated K^+ channel ($K_{Ca}3.1$, $IK_{Ca}1$); $I_{K(A)}$, transient A-type K^+ current; $I_{BK(Ca)}$, Ca^{2+}-activated K^+ channel current; $I_{K(DR)}$, delayed-rectifier K^+ current; α-KTx, potassium channel scorpion toxin; K_V channel, voltage-activated K^+ channel; M-LVA, mid- to low-voltage-activated; NIS, normal insect saline; SK_{Ca} channel, small-conductance Ca^{2+}-activated K^+ channel ($K_{Ca}2.x$); TEA, tetraethylammonium; TRTX, theraphotoxin (from the venom of spiders belonging to the family Theraphosidae); TTX, tetrodotoxin; HPLC, high-performance liquid chromatography; TFA, trifluoroacetic acid; RP-HPLC, reversed-phase high-performance liquid chromatography; ICK, inhibitor cystine knot; *f*, fraction.

insect-selective lead compounds would therefore provide a fresh approach in the development of more effective insect control agents.

It is already well established that ion channel toxins, particularly those targeting voltage-activated sodium (Na_V) channels, are useful insecticidal compounds, given their rapid lethal activity, high potency, and relative insect selectivity. Nevertheless, with an increasing incidence of insecticide resistance, there is a need to explore novel targets, such as insect voltage-activated calcium (Ca_V) and potassium (K_V) channels (King et al., 2008a). It is noteworthy that potassium channels are a diverse group of ion channels represented in both electrically excitable and nonexcitable tissues and as such represent a novel target mediating the effects of potential insecticidal agents.

Peptide toxins isolated from spider venoms have long been recognized as valuable pharmacological tools for probing mammalian voltage-activated ion channel structure and function (Swartz, 2007). However, attention has been turning to their use as potential sources of insecticidal agents. The evolutionary process in spiders has led to the development of rich combinatorial peptide libraries, mostly comprising ion channel toxins specifically designed to rapidly immobilize and kill insect prey (Escoubas, 2006; King et al., 2008a). Indeed, recent evidence would suggest that some venoms from "primitive" mygalomorph spiders contain more than 1000 peptides (Escoubas et al., 2006). Although mygalomorph venoms potentially contain toxins for a wide range of insect targets, it is likely that toxins targeting voltage-activated ion channels are mainly responsible for the fast lethal effects of these venoms in insects. It is this rapid and pernicious insect-selective activity that makes these toxins ideal candidates as leads for the design of novel insecticides.

κ-Hexatoxin-Hv1c (κ-HXTX-Hv1c, formerly J-atracotoxin-Hv1c; King et al., 2008b) from the venom of the Australian funnel-web *Hadronyche versuta* (Araneae: Mygalomorphae: Hexathelidae) has been identified as the first toxin to selectively and potently target an insect K^+ channel, with selective actions to block insect but not vertebrate large-conductance BK_{Ca} channels (Gunning et al., 2008). κ-HXTX-Hv1c exhibits lethal activities in a number of insect orders, including Coleoptera, Diptera, Lepidoptera, and Orthoptera, whereas lacking activity in mouse, rabbit, rat, and chick preparations (Maggio and King, 2002). Thus κ-HXTX-Hv1c validates K^+ channels as potential insecticidal targets.

Although several insect-selective toxins have been isolated from the venom of spiders belonging to the family Hexathelidae (King, 2007; Nicholson, 2007b), there has been only a limited number of investigations of insecticidal toxins from spiders of the family Theraphosidae (Li et al., 2003; Corzo et al., 2008). This is despite a number of toxins from theraphosid ("tarantula") spiders targeting mammalian acid-sensing ion channels, mechanosensitive, K_V, Na_V, and Ca_V channels having been characterized (see the ArachnoServer 2.0 Spider Toxin Database, http://www.arachnoserver.org/) (Herzig et al., 2011). In this study, we describe a family of toxins (theraphotoxins) from the venom of the East African tarantula *Eucratoscelus constrictus* (Gerstäcker 1873; Araneae: Mygalomorphae: Theraphosidae) that block insect BK_{Ca} channels and fail to significantly affect other insect K_V, Na_V, and both mid- to low-voltage-activated (M-LVA) and high-voltage-activated (HVA) Ca_V channels. It is noteworthy that although these toxins share their target with κ-HXTX-Hv1c, they possess no obvious sequence homology, implying that they may interact with distinct portions of the insect BK_{Ca} channel. These theraphotoxins will be useful for probing the biological role of BK_{Ca} channels in insects and are potential lead compounds for the development of insect-selective biopesticides.

Materials and Methods

Venom Supply. *E. constrictus* (formerly *E. longiceps*; World Spider Catalog, http://research.amnh.org/entomology/spiders/catalog/index.html) venom was purchased from a commercial supplier (Invertebrate Biologics, Los Gatos, CA). Venom was obtained using electrical stimulation of the chelicera. Crude venom was first diluted up to two thirds of its final volume in ultrapure distilled water, centrifuged at 14,000 rpm for 30 min at 4°C, and filtered using a 0.45-μm microfilter (Millipore Corporation, Billerica, MA). The filter was rinsed with water (one third of final volume), and the venom was diluted to 10 times its initial volume and stored at −20°C until further use.

Toxin Purification and Biochemical Characterization. Bioassay-guided fractionation of *E. constrictus* venom was performed using both reversed-phase and cation-exchange high-pressure liquid chromatography (HPLC). A volume of 20 to 25 μl of crude venom equivalent was diluted with 0.1% aqueous trifluoroacetic acid (TFA) and fractionated by reversed-phase HPLC (RP-HPLC) on a semi-preparative C8 column (10 × 250 mm; Nacalai Tesque, Kyoto, Japan). The column was equilibrated in 0.1% TFA, and peptides were eluted with a 5 to 60% acetonitrile/0.1% TFA gradient at a flow rate of 2 ml/min (see Fig. 2 for details). Fractions were collected manually by monitoring the absorbance at 215 nm. The fractions were vacuum-dried, dissolved in 200 μl of ultrapure water, and tested for insecticidal activity (see below). Insecticidal fractions were further purified by cation-exchange HPLC using a TSKgel sulfopropyl column (4.6 × 75 mm; Tosoh Corporation, Tokyo, Japan). The fractions were diluted to 200 μl with 20 mM ammonium acetate and were analyzed using a linear gradient from 20 mM to 2 M ammonium acetate at 0.5 ml/min (see Fig. 2 for details). Absorbance was monitored at 280 nm, and fractions were collected manually. Fractions were dried under vacuum, and a final purification step was undertaken using an RP-HPLC C18 column (4.6 × 250 mm; Waters Symmetry, Waters, Milford, MA) and a water/acetonitrile/0.1% TFA gradient at 1 ml/min (see Fig. 2 for details). Purified toxins were freeze-dried and stored at −20°C.

Insect Lethality Assays. Juvenile crickets (*Gryllus bimaculatus* third instar nymphs; average weight, 65–70 mg) were injected intrathoracically with 1 to 5 μl using a 10-μl precision syringe. Samples were dissolved in distilled water, and controls were injected with water only. For more rapid toxin identification, pools of fractions were tested. Each RP-HPLC fraction (see below) was dried, reconstituted in 200 μl of distilled water, and 1-μl aliquots of each fraction were mixed to reconstitute pools of 8 to 10 fractions. Final pool volumes varied from 8 to 14 μl depending on the number of aliquots mixed for a given pool. 2 μl of each pool was injected into crickets as described above ($n = 3$). For individual RP-HPLC fractions, aliquots of 1 μl were diluted 10 times in distilled water, and 2 μl was injected into crickets ($n = 3$). Cation-exchange HPLC fractions were freeze-dried, redissolved in distilled water, and 1:20 aliquots were injected into crickets ($n = 3$). Observation of paralysis and/or death was made at 5, 15, and 60 min after injection with the assay endpoint for calculation of median effective doses (ED_{50}) being 15 min. ED_{50} values were evaluated using a range of five to six venom or toxin concentrations, with five crickets per dose ($n = 3$). Results were analyzed using the SOFTTOX program (WindowChem, Fairfield, CA) using the probit analysis method.

Mouse Bioassays. Activity against vertebrates was evaluated by intracerebroventricular injection in female C57BL/6 mice. Mice (approximately 20 g average weight) were lightly anesthetized with diethyl ether, injected in the left cerebral ventricle with 5 μl of sample dissolved in a solution of bovine serum albumin [2% (w/v) in saline], and placed in glass jars for observation. Development of signs of toxicity was noted continuously during the first hour after injection and was monitored at regular intervals for 24 h or until death. A dose of 500 pmol/mouse was used to discriminate insect-selective peptides from peptides with both insect and vertebrate activity ($n = 2$).

Edman Peptide Sequencing. Before sequencing, toxins were reduced with 20 mM β-mercaptoethanol (30 min, 37°C) and were alkylated with 4-vinylpyridine (Wako Pure Chemicals, Osaka, Japan), in 250 mM Tris-HCl/6 M guanidine buffer, pH 8.3, for 30 min at 37°C in the dark under argon. The pyridylethylated toxins were desalted by C18 RP-HPLC using a linear gradient of acetonitrile/water/0.1% TFA. Toxin sequencing was performed on an Applied Biosystems 477A automated gas-phase sequencer (Applied Biosystems, Foster City, CA). Pyridylethylated toxins were dissolved in HPLC-grade water, applied to TFA-treated glass fiber membranes precycled with Biobrene (Applied Biosystems), and subjected to N-terminal (Edman) sequencing. Sequence homologies were determined from a BLAST search of the ArachnoServer 2.0 Spider Toxin Database server.

Mass Spectrometry. Mass spectra were recorded on an Applied Biosystems Voyager DE-Pro matrix-assisted laser desorption/ionization time-of-flight mass spectrometer (Applied Biosystems), in positive ion linear or reflector mode using α-cyano-4-hydroxycinnamic acid matrix. Calibrations were performed either in close external or internal mode, with a mixture of synthetic peptide calibrants (LaserBio Labs, Sophia-Antipolis, France). Data were analyzed with the manufacturer's DATA EXPLORER software. To confirm sequencing data, trypsin cleavage of κ-TRTX-Ec2b was performed in Tris-HCl buffer, pH 8.5, at 37°C for 4 h, with a 1:50 enzyme-to-peptide ratio. Trypsin was purchased from Promega (Charbonnières-les-Bains, France). Theoretical molecular masses were then calculated with version 7.10 of the GPMAW program (http://www.gpmaw.com/index.html) and compared with measured masses.

Homology Modeling. Three-dimensional models of the κ-TRTX-Ec2 toxins were calculated using the NMR structure coordinates of κ-TRTX-Gr2a (Protein Data Bank ID 1LUP) as a template via submission to the Swiss Model server (http://www.expasy.ch/swissmod/SWISS-MODEL.html) and analyzed with PYMOL software version 1.3 (http://www.pymol.org).

Patch-Clamp Electrophysiology. Whole-cell currents were recorded in voltage-clamp mode using the whole-cell patch-clamp technique using version 9 of the pCLAMP data acquisition system (Molecular Devices, Sunnyvale, CA). Data were filtered at 5 kHz with a low-pass Bessel filter with leakage and capacitative currents subtracted using P-P/4 procedures. Digital sampling rates were set between 15 and 25 kHz depending on the length of the voltage protocol. Using a Flaming-Brown micropipette puller (Sutter Instrument Company, Novato, CA), single-use electrodes were pulled from borosilicate glass to direct current resistances of approximately 1, 1.5, and 2.5 MΩ for sodium, calcium, and potassium channel current recordings, respectively. Liquid junction potentials for the various combinations of internal pipette and external bath solutions were calculated using the JPCalc software program (Molecular Devices), and all data were compensated for these values. Series resistance compensation was >80% for all cells. Cells were bathed in external solution through a continuous pressurized perfusion system at 1 ml/min, whereas toxin solutions were introduced via direct pressurized application via a perfusion needle at approximately 50 μl/min (Automate Scientific, San Francisco, CA). All experiments were performed at ambient room temperature (20–23°C).

Primary Cell Culture. Dorsal unpaired median (DUM) neurons were isolated from unsexed adult American cockroaches (*Periplaneta americana*) as described previously (Gunning et al., 2008). In brief, DUM neurons were enzymatically and mechanically isolated from the terminal abdominal ganglia of the cockroach. Extracted ganglia were removed and placed in normal insect saline (NIS) containing 180 mM NaCl, 3.1 mM, 10 mM HEPES, and 20 mM D-glucose. Ganglia were then incubated in 1 mg/ml collagenase (type IA) for 40 min at 29°C. After enzymatic treatment, ganglia were washed three times in NIS and triturated through a fire-polished pipette to dissociate individual neurons. The cell suspension was then distributed onto 12-mm diameter glass coverslips precoated with 1 mg/ml concanavalin A (type IV). Cells were maintained for no longer than 24 h in NIS supplemented with 5 mM $CaCl_2$, 4 mM $MgCl_2$, 5% fetal bovine serum, and 1% penicillin and streptomycin and maintained at 30°C, 100% humidity.

Electrophysiological Recording Solutions. To record I_{Na}, the external bath solution contained 80 mM NaCl, 5 mM CsCl, 1.8 mM $CaCl_2$, 50 mM tetraethylammonium (TEA) chloride, 5 mM 4-aminopyridine (4-AP), 10 mM HEPES, 0.1 mM $NiCl_2$, and 1 mM $CdCl_2$, adjusted to pH 7.4 with 1 M NaOH. The pipette solution contained 34 mM NaCl, 135 mM CsF, 1 mM $MgCl_2$, 10 mM HEPES, 5 mM EGTA, and 3 mM ATP-Na_2, adjusted to pH 7.4 with 1 M CsOH.

Because of the report of I_{Ca} rundown with calcium as a charge carrier and greater success when barium was used as the charge carrier (Wicher and Penzlin, 1997), $BaCl_2$ replaced $CaCl_2$ in all experiments. The external bath solution for barium current (I_{Ba}) recordings contained 140 mM sodium acetate, 30 mM TEA-bromide, 3 mM $BaCl_2$, and 10 mM HEPES, adjusted to pH 7.4 with 1 M TEA-OH. The external solution also contained 300 nM tetrodotoxin (TTX) to block Na_V channels. Pipette solutions contained 10 mM sodium acetate, 110 mM CsCl, 50 mM TEA-bromide, 2 mM ATP-Na_2, 0.5 mM $CaCl_2$, 10 mM EGTA, and 10 mM HEPES, adjusted to pH 7.4 with 1 M CsOH.

The external bath solution for recording macroscopic K_V channel currents contained 150 mM NaCl, 30 mM KCl, 5 mM $CaCl_2$, 4 mM $MgCl_2$, 0.3 mM TTX, 10 mM HEPES, and 10 mM D-glucose, adjusted to pH 7.4 with 1 M NaOH. The pipette solution consisted of 135 mM KCl, 25 mM KF, 9 mM NaCl, 0.1 mM $CaCl_2$, 1 mM $MgCl_2$, 1 mM EGTA, 10 mM HEPES, and 3 mM ATP-Na_2, adjusted to pH 7.4 with 1 M KOH.

To eliminate any influence of differences in osmotic pressure, all internal and external solutions were adjusted to 400 ± 5 mOsM with sucrose. Experiments were rejected if there were large leak currents or currents showed signs of poor space clamping.

Curve-Fitting and Statistical Analysis. Data analyses were completed offline at the conclusion of experiments using AxoGraph X version 1.1 (Molecular Devices). Mathematical curve-fitting was accomplished using PRISM version 5.00b for Macintosh (GraphPad Software Inc., San Diego, CA). All curve-fitting routines were performed using nonlinear regression analysis using a least-squares method. Comparisons of two sample means were made using a paired Student's t test. Multiple comparisons were assessed by repeated-measures analysis of variance with a Bonferroni's multiple comparison post hoc test; differences were considered to be significant if $p < 0.05$. All data are presented as mean ± S.E.M. of n independent experiments, unless stated otherwise.

The following equation was employed to fit current-voltage curves:

$$I = g_{max}\left(1 - \left(\frac{1}{1 + \exp[(V - V_{1/2})/s]}\right)\right)(V - V_{rev})$$

where I is the amplitude of the peak current (either I_{Ba}, I_{Na}, or I_K) at a given test potential V, g_{max} is the maximal conductance, $V_{1/2}$ is the voltage at half-maximal activation, s is the slope factor, and V_{rev} is the reversal potential. Concentration-response curves were fitted using the following logistic equation:

$$y = \frac{1}{1 + ([x]/IC_{50})^{n_H}}$$

where x is the toxin dose, n_H is the Hill coefficient (slope parameter), and IC_{50} is the median inhibitory concentration to block channel currents.

Results

Purification of Insecticidal Neurotoxins. As part of a search for novel insecticidal peptide toxins, a large-scale screening of theraphosid venoms was pursued. Venom extracted from the African "tarantula" *E. constrictus* was selected for its particularly potent paralytic activity in crickets (ED_{50} = 0.017 μl/g; Fig. 1). Bioassay-guided fractionation of crude *E. constrictus* venom by C8 RP-HPLC yielded 26 fractions, with fraction 14 (*f*14) being selected for its high insecticidal toxicity (Fig. 2A). Because fractions *f*14 to *f*16 were inadequately resolved in the first HPLC separation, they were pooled and analyzed together by cation-exchange HPLC (Fig. 2B). This led to the separation of seven fractions (*f*14.1-*f*14.7) that were then tested for insect and mammalian activity. These seven fractions yielded three insecticidal peptides (*f*14.2, *f*14.3, and *f*14.5), which were fully purified after an additional chromatography step using C18 RP-HPLC (Fig. 2C). In the insect assay, all three fractions demonstrated significant neurotoxicity at a dose of 1.1 nmol/g (4 μg/g). At this dose, the three toxins caused rapid insecticidal activity, with complete paralysis within 5 min, and death within 15 min (n = 3). For *f*14.2 and *f*14.3, intracerebroventricular injection of 500 pmol (1.8 μg) into 20-g mice (n = 2) also did not result in any neurotoxicity or behavioral symptoms. All aspects of mouse posture and behavior appeared to be totally unaffected by toxin injection, indicating that *f*14.2 and *f*14.3 are phyla-selective neurotoxins. On the other hand, injection of 500 pmol *f*14.5 (1.8 μg) into 20-g mice (n = 2) resulted in strong neurotoxicity symptoms, including convulsions, tonic paralysis, general ataxia, extension of legs and toes, tail erection, and respiratory paralysis resulting in very marked cyanosis of the animal. These symptoms seemed to be reversible because animals recovered from cyanosis and tonic paralysis after approximately 4 h and started to resume normal posture and activity.

Edman degradation of reduced and alkylated peptides yielded the complete N-terminal sequence of the three toxins from single sequencing runs. All cysteine residues were definitively established after reduction and alkylation using 4-vinylpyridine. Based on their mass and amino acid sequence, these toxins belong to a class of inhibitor cystine knot (ICK) toxins (Pallaghy et al., 1994) with six cysteines (C_I–C_{VI}). The κ-TRTX-Ec2 toxins also clearly belong to the family of "short-loop" ICK spider peptides, distinguished from the more common "long-loop" ICK spider toxins, by the presence of only three residues in the C_V–C_{VI} loop (Escoubas and Rash, 2004). Because of high homology with a number of other previously characterized short-loop tarantula, we propose the presence of three disulfide bonds (Fig. 3A) linked in the C_I–C_{IV}, C_{II}–C_V, and C_{III}–C_{VI} pattern resulting in a disulfide-linked pseudoknot described previously for this toxin family.

To verify sequencing data, *f*14.3 was also digested with trypsin and the resulting peptide mixture analyzed with matrix-assisted laser desorption/ionization time-of-flight mass spectrometry for confirmation of sequence ambiguities, particularly the presence of Trp24. In addition, the measured masses of the peptides were matched with calculated theoretical mass values of the amino acid sequence, using the software program GPMAW (http://www.gpmaw.com/). This allowed complete unambiguous sequence confirmation (data not shown).

Each peptide consists of 29 amino acids with observed monoisotopic molecular masses of 3626.73, 3676.71, and 3627.16 Da for *f*14.2, *f*14.3, and *f*14.5, respectively. This compares very well with the monoisotopic mass predicted from the sequence of 3626.53, 3676.51, and 3627.52 Da, respectively. This indicates that there are no apparent post-translational modifications, such as C-terminal amidation, observed with certain other spider toxins (e.g., β-TRTX-Gr1b, formerly GsAFI; see Fig. 3A). The three toxins share more than 80% sequence homology with a number of spider toxins, the majority of which are short-loop toxins from the venom of another theraphosid spider, *Grammostola rosea* (Fig. 3A). Homologous peptides exhibited a range of activities including high-affinity inhibition of Na_V, $Ca_V1.2$, $Ca_V3.1$, $K_V4.1$, $K_V4.2$, $K_V4.3$, and K_VAP channels and weak affinity for mechanosensitive and $K_V2.1$ channels (see the ArachnoServer 2.0 database for a full list of references). Furthermore, the positions of all cysteines were strictly conserved with all short-loop theraphosid spider toxins (Fig. 3A).

Using the rational nomenclature system for spider toxins proposed by King et al. (2008), *f*14.2, *f*14.3, and *f*14.5 were named κ-theraphotoxin (TRTX)-Ec2a, κ-TRTX-Ec2b, and κ-TRTX-Ec2c, respectively. The activity descriptor prefix "κ" indicates modulators of K^+ channels (evidence presented

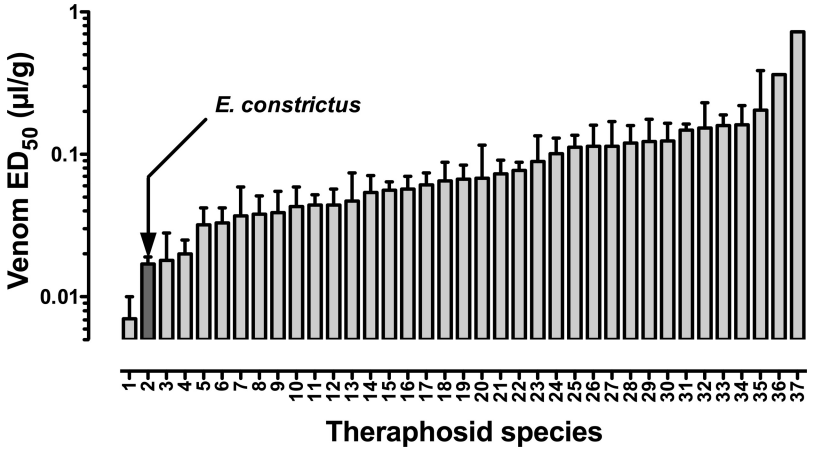

Fig. 1. Insecticidal toxicity screening of tarantula venoms in *G. bimaculatus* crickets. ED_{50} values for paralysis at 15 min after intrathoracic injection were calculated by the probit method and are expressed as microliters of crude venom per gram of insect. Values represent the mean ± 95% confidence limits with n = 3 in all cases, except species 36 and 37, where n = 1 as a result of lack of potency and availability of venom.

below), "theraphotoxin" is the generic name for toxins from the family Theraphosidae (see Supplemental Table 4 in King et al., 2008b), "Ec" is the genus and species descriptor for *E. constrictus*, 2 is consistent with the majority of other short-loop ICK tarantula toxins (see below), and *a*, *b*, and *c* denote the first three paralogs (isoforms) discovered.

Target Determination of κ-TRTX-Ec2 Toxins. Although κ-TRTX-Ec2 toxins share a similar sequence and cysteine spacing arrangement with short-loop theraphotoxins, this provided few clues as to the potential target of κ-TRTX-Ec2 toxins. This is because within the short-loop theraphotoxin group, the biological activities are quite diverse with activities on a wide variety of voltage-activated and mechanosensitive ion channel targets. Nevertheless, given the considerable sequence homology of κ-TRTX-Ec2 toxins with β-TRTX-Gr1a (formerly GrTx-I) from *G. rosea* (Fig. 3A), a toxin known to target mammalian Na_V channels, initial experiments investigated whether κ-TRTX-Ec2 toxins modulated insect Na_V channel currents (I_{Na}). Whole-cell TTX-sensitive I_{Na} were recorded from cockroach DUM neurons in the voltage-clamp configuration. Test pulses to −10 mV (Fig. 4D) from a holding potential (V_h) of −90 mV elicited a fast activating and inactivating inward I_{Na} that could be abolished by the addition of 300 nM TTX (Fig. 4A). The application of 330 nM κ-TRTX-Ec2b failed to significantly alter I_{Na} amplitude or time course over a 10-min perfusion period (92 ± 4% of control peak I_{Na}, $p > 0.05$, $n = 3$; Fig. 4A).

Experiments then investigated whether κ-TRTX-Ec2 toxins modulated the activity of insect Ca_V channels. This was based on their significant sequence homology with β/ω-TRTX-Tp2a (formerly ProTx-II) from *Thrixopelma pruriens* (Fig. 3A) shown previously to target mammalian $Ca_V1.2$ and $Ca_V3.1$ channels, as well as Na_V channels (Middleton et al., 2002; Edgerton et al., 2007). We investigated the action of κ-TRTX-Ec2 toxins on both HVA and M-LVA Ca_V channels that have been characterized previously in cockroach DUM

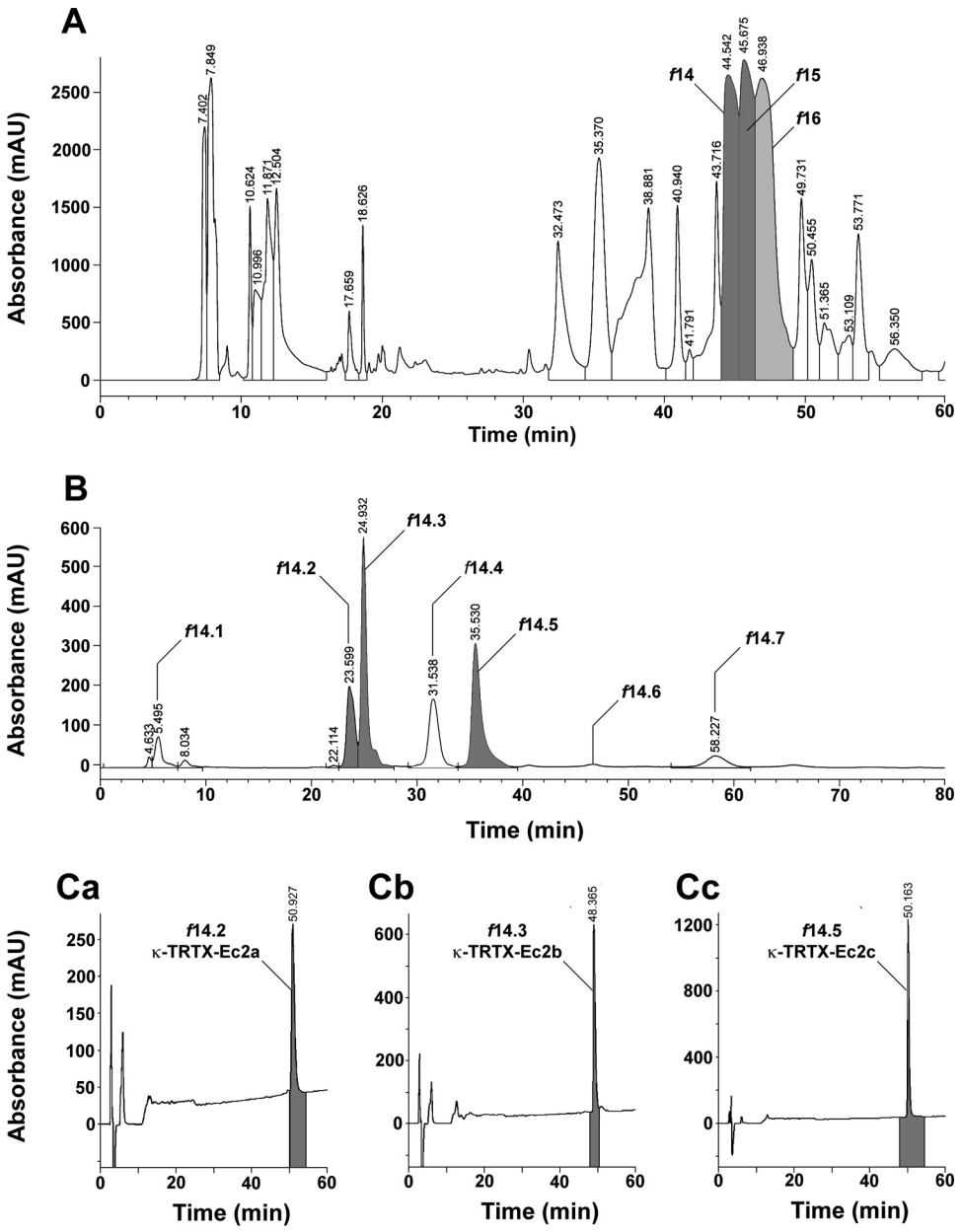

Fig. 2. Isolation and purification of κ-TRTX-Ec2 toxins. A, C8 RP-HPLC of crude *E. constrictus* venom (20 μl). Gradient: 0% B, 5 min; 0 to 15% B, 15 min; 15 to 50% B, 70 min; 50 to 60% B, 10 min; 60 to 90% B, 5 min; and 90 to 0% B, 5 min. A, H_2O/0.1% TFA; B, acetonitrile/0.1% TFA, 2 ml/min. Eluted peptides were monitored at an absorbance of 215 nm. B, cation exchange HPLC of pooled fractions 14 to 16 (*f*14) from C8 RP-HPLC (shaded peaks in A). Gradient: 0% B, 10 min; 0 to 50% B, 50 min; 50 to 100% B, 15 min; and 100 to 0% B, 15 min. A, 20 mM ammonium acetate; B, 2 M ammonium acetate, 0.5 ml/min. Eluted peptides were monitored at an absorbance of 280 nm. C, C18 RP-HPLC purification of fractions *f*14.2 (κ-TRTX-Ec2a, Ca), *f*14.3 (κ-TRTX-Ec2b, Cb), and *f*14.3 (κ-TRTX-Ec2c, Cc) from cation-exchange HPLC (shaded peaks in B). Gradient: 0% B, 5 min; 0 to 15% B, 15 min; 15 to 40% B, 50 min; 40 to 90% B, 10 min; and 90 to 0% B, 5 min. A, H_2O/0.1% TFA; B, acetonitrile/0.1% TFA, 1 ml/min. Eluted peptides were monitored at an absorbance of 215 nm. In each, retention times (in minutes) are shown above each peak.

neurons (Chong et al., 2007). Unfortunately, despite differences in the kinetic and pharmacological properties of M-LVA and HVA Ca_V channels, there remains no mechanism for recording one current in isolation from the other because no peptide or organic blockers are available that exclusively block one channel subtype. As described previously, depolarizing pulses to two potentials (−20 and +30 mV; Fig. 4D) from a V_h of −90 mV were used to investigate the actions of the κ-TRTX-Ec2 toxins on M-LVA and HVA Ca_V channels, respectively (Chong et al., 2007). The elicited barium current (I_{Ba}) was abolished by the addition of 1 mM $CdCl_2$, confirming that currents were carried via Ca_V channels (Fig. 4Ba). A 10-min application of 330 nM κ-TRTX-Ec2b failed to significantly reduce either M-LVA or HVA Ca_V channel currents, with only a 10 ± 6% ($p > 0.05$, $n = 3$) and 7 ± 6% ($p > 0.05$, $n = 3$) inhibition of control peak I_{Ba}, respectively (Fig. 4B, a and b).

To determine whether κ-TRTX-Ec2 toxins alter the voltage-dependence of channel activation, voltage protocols from a V_h of −90 to +70 mV in 10-mV increments were delivered at a frequency of 0.1 Hz to elicit families of I_{Na} and I_{Ba}. Resultant peak I_{Na}-V and peak I_{Ba}-V relationships were fitted with eq. 1 (see *Materials and Methods*). Consistent with a lack of inhibition of I_{Na} or I_{Ba} amplitude, there was no significant shift in the threshold, or voltage midpoint, of activation ($V_{1/2}$) of Na_V or Ca_V channels in the presence of 330 nM toxin (data not shown). These experiments therefore indicate that κ-TRTX-Ec2 toxins fail to affect invertebrate Na_V and Ca_V channels in the model studied.

Global K_V channel currents were recorded in the presence of 300 nM TTX and 1 mM $CdCl_2$ to block Na_V and Ca_V channel currents, respectively. Currents were elicited by depolarizing test pulses to +30 mV (Fig. 4D) and upon the addition of 50 mM TEA-chloride, a nonselective K_V blocker, the channel current was completely abolished indicating that these currents were carried by K^+ channels (data not shown). In contrast to the lack of overt activity on insect Ca_V and Na_V channels, a 10-min perfusion with 330 nM κ-TRTX-Ec2a, -Ec2b, or -Ec2c resulted in a significant reduction in DUM neuron global K_V channel current amplitude (Fig. 4C). This effect was partially reversible with approximately 50% recovery observed after a 10-min washout with toxin-free external solution.

Determining the K^+ Channel Subtype Specificity of κ-TRTX-Ec2 Toxins. Block of global outward I_K indicates that κ-TRTX-Ec2 toxins target at least one of the four major K^+ channel current subtypes in cockroach DUM neurons. These are identified according to their current kinetics and pharmacological properties and include slowly activating, noninactivating delayed-rectifier [$I_{K(DR)}$], transient "A-type" [$I_{K(A)}$], transient Na^+-activated [$I_{K(Na)}$], as well as large-conductance "late-sustained" and "fast-transient" Ca^{2+}-activated [$I_{BK(Ca)}$] K^+ channel currents (Grolleau and Lapied, 1995). The fast-transient BK_{Ca} channel differs from the late-sustained BK_{Ca} channel in that it inactivates rapidly after activation and displays a voltage-dependent resting inactivation (Grolleau and Lapied, 1995). The K_{Ca} current in cockroach DUM neurons is of the large-conductance (BK_{Ca}) subtype because the current is voltage-activated, whereas SK_{Ca} and IK_{Ca} channel currents are voltage-insensitive, and no apamin-sensitive SK_{Ca} channels have been found in isolated cockroach DUM neurons (Grolleau and Lapied, 1995). As a consequence of the inhibition of macroscopic outward I_K, all subtypes except for K_{Na} channels, which contribute only a

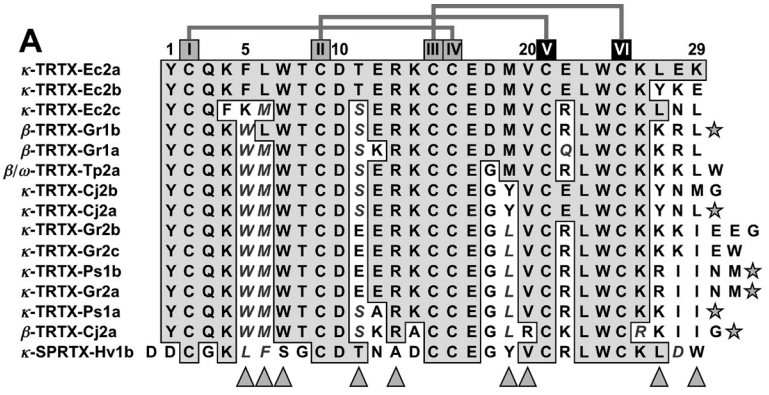

% I	% H	Target	Former Name	Source
100	100	BK_{Ca} (K_{DR}) insect	–	*E. constrictus*
90	90	BK_{Ca} insect	–	*E. constrictus*
76	83	BK_{Ca} insect	–	*E. constrictus*
79	86	Na_V	GsAFI	*Grammostola rosea*
72	86	Na_V	GrTx1	*Grammostola rosea*
72	83	Na_V, $Ca_V1.2$, $Ca_V3.1$	ProTx-II	*Thrixopelma pruriens*
72	83	$K_V4.1$ ($K_V4.2$, $K_V2.1$)?	JZTX-46	*Chilobrachys jingzhao*
72	83	$K_V4.1$ ($K_V4.2$, $K_V2.1$)	JZTX-XII	*Chilobrachys jingzhao*
69	80	K_VAP (MSC?)	VSTX2	*Grammostola rosea*
69	80	K_VAP? (MSC)	GsAFII	*Grammostola rosea*
69	80	$K_V4.2$, $K_V4.3$ (MSC)	PaTx2	*Paraphysa scrofa*
69	80	$K_V4.2$, $K_V4.3$ (MSC)	GsMTx-2	*Grammostola rosea*
66	80	$K_V4.2$, $K_V4.3$	PaTx1	*Paraphysa scrofa*
55	72	Na_V ($K_V4.2$, $K_V4.3$)	JZTX-V	*Chilobrachys jingzhao*
52	62	$K_V4.2$, $K_V4.3$ ($K_V4.1$)	HPTX2	*Heteropoda venatoria*

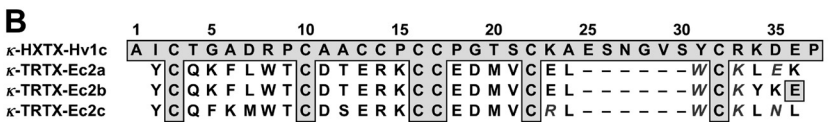

% H	Target	Former Name	Source
100	BK_{Ca} (K_A) insect	J-ACTX-Hv1c	*Hadronyche versuta*
31	BK_{Ca} (K_{DR}) insect	–	*E. constrictus*
31	BK_{Ca} insect	–	*E. constrictus*
34	BK_{Ca} insect	–	*E. constrictus*

Fig. 3. Homology of κ-TRTX-Ec2 toxins with short-loop ICK spider toxins. A, a Blast search was run through the ArachnoServer 2.0 Database highlighting peptides with highly homologous sequences. All sequences belong to the short-loop ICK group of tarantula toxins defined by three residues in the loop between the highlighted C_V and C_{VI} cysteine residues (Escoubas and Rash, 2004). Homologies are shown relative to κ-TRTX-Ec2a; identities are boxed in gray, whereas conservative substitutions are in gray italic text. Stars represent C-terminal amidation. Percentage identity (%I) is relative to κ-TRTX-Ec2a, whereas percentage homology (%H) includes conservatively substituted residues. The disulfide bonding pattern for the strictly conserved cysteine residues determined for κ-TRTX-Gr2a (Oswald et al., 2002) and κ-TRTX-Ps2a (Diochot et al., 1999) is indicated above the sequences; it is assumed that the κ-TRTX-Ec2 toxins share the same disulfide bonding pattern. The known mammalian targets (unless otherwise indicated) of these spider toxins are identified on the right, with channels identified in brackets indicating only weak affinity. Those targets annotated with a question mark indicate a likely target based on considerable homology with a toxin of known pharmacology (e.g., κ-TRTX-Gr2b and κ-TRTX-Gr2c). It is noteworthy that κ-TRTX-Ps2b and κ-TRTX-Gr2a possess identical sequences, although they originate from unrelated species. Sequence, post-translational modifications, disulfide connectivity, and pharmacological target data were obtained from the ArachnoServer 2.0 database. B, despite sharing a similar phyla and target selectivity, κ-TRTX-Ec2 toxins show only limited homology to κ-HXTX-Hv1c (Gunning et al., 2008). Gaps (dashes) have been inserted to maximize alignment.

minor portion of the total current, were investigated as potential targets of κ-TRTX-Ec2 toxins.

For isolation of K^+ channel subtypes, various channel blockers and current subtraction routines were used. To isolate outward $I_{K(DR)}$ in DUM neurons, $I_{K(A)}$ were blocked with 5 mM 4-AP (Grolleau and Lapied, 1995; Gunning et al., 2008) whereas BK_{Ca} channels were blocked with 1 mM $CdCl_2$ and 30 nM charybdotoxin (ChTx) (Gunning et al., 2008). Both κ-TRTX-Ec2b and κ-TRTX-Ec2c (330 nM) failed to significantly inhibit $I_{K(DR)}$ ($p > 0.05$, $n = 3$; Fig. 5C b and c). However κ-TRTX-Ec2a produced a 31 ± 12% inhibition of control $I_{K(DR)}$ ($p < 0.01$, $n = 3$; Fig. 5Ca). To assess whether κ-TRTX-Ec2 toxins alter the voltage-dependence of $I_{K(DR)}$ activation, the current-voltage [$I_{K(DR)}$-V] relationship in the presence of each toxin was determined using a series of 100-ms voltage pulses from a V_h of −90 to +40 mV in 10-mV increments, delivered at a frequency of 0.2 Hz. The threshold of $I_{K(DR)}$ activation was at membrane potentials more depolarized than −50 mV, in agreement with previous data from $I_{K(DR)}$ recordings in DUM neurons (Grolleau and Lapied, 1995; Gunning et al., 2008). Data were normalized against maximal late current (measured at 100 ms) recorded in the absence of toxin and subsequently fitted with eq. 1 (see *Materials and Methods*). It is noteworthy that there were no significant shifts in the voltage-dependence of $I_{K(DR)}$ activation for any κ-TRTX-Ec2 toxin ($\Delta V_{1/2} < 5.5$ mV for all toxins, $p > 0.05$, $n = 3$–7) (Fig. 5D). In summary, κ-TRTX-Ec2b and κ-TRTX-Ec2c failed to significantly inhibit $I_{K(DR)}$, although in the case of κ-TRTX-Ec2a, this may account for a statistically significant proportion of the block of global K_V current (Fig. 4C).

In insects, the *shaker*, *shab*, *shaw,* and *shal* genes encode for the equivalents of mammalian K_V1–K_V4 channels, respectively. Although it is believed the Shab and Shaw channels are responsible for $I_{K(DR)}$ in insects (Wei et al., 1990), little work has been done on native neurons, apart from *Drosophila melanogaster* to determine the various contributions of these two channels. Therefore, it is quite possible that κ-TRTX-Ec2a targets, with moderate affinity, one of the two possible K_V channel subtypes contributing to $I_{K(DR)}$. However, at present, the relative expression of Shab versus Shaw channel subtypes in cockroach DUM neurons is unknown, and given the potent action on BK_{Ca} channels (see below), such an action is unlikely to contribute significantly to the overall activity of κ-TRTX-Ec2a.

Of particular interest was the effect of κ-TRTX-Ec2 toxins on $I_{K(A)}$ as a result of their homology with a number of theraphosid spider toxins targeting the mammalian K_V4 channel (Fig. 3A). The K_V4 channel is the ortholog of the insect Shal channel that is believed to underlie a significant portion of the $I_{K(A)}$ (Salkoff et al., 1992). $I_{K(A)}$ cannot be recorded in isolation from $I_{K(DR)}$ because there are no selective blockers of insect $I_{K(DR)}$. To record $I_{K(A)}$ in isolation from other K_V channel currents, a subtraction routine was therefore employed using 4-AP. To isolate $I_{K(A)}$, neurons were continuously perfused with 30 nM ChTx and 1 mM $CdCl_2$ to block BK_{Ca} channels (Gunning et al., 2008). At the conclusion of experiments, 5 mM 4-AP was then perfused to eliminate $I_{K(A)}$, allowing for offline subtraction of the remaining $I_{K(DR)}$. This involved separate experiments with κ-TRTX-Ec2a, -Ec2b, or -Ec2c, which were perfused for a period of 10 min or until equilibrium was achieved. 4-AP (5 mM) was then ap-

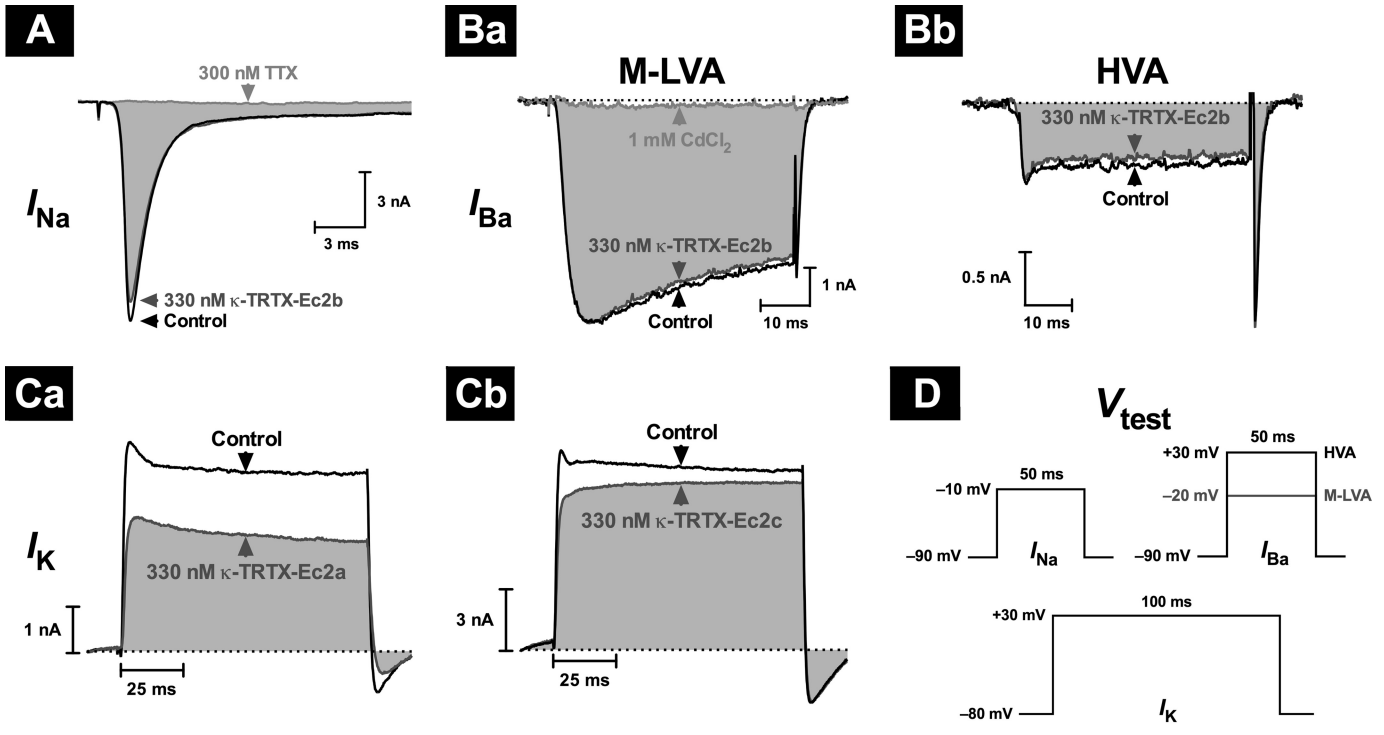

Fig. 4. Effects of κ-TRTX-Ec2 toxins on whole-cell Na_V, Ca_V, and macroscopic K_V channel currents in cockroach DUM neurons. A and B, representative superimposed current traces showing the lack of a significant effect of 330 nM κ-TRTX-Ec2 toxins on Na_V channel currents (A), LVA-Ca_V channel currents (Ba), or HVA-Ca_V channel currents (Bb). Note the block of all residual I_{Na} and I_{Ba} by 300 nM TTX and 1 mM Cd^{2+}, respectively. C, superimposed current traces demonstrating the typical effect of κ-TRTX-Ec2a (Ca) and κ-TRTX-Ec2c (Cb) on macroscopic K_V channel currents. D, depolarizing voltage test pulse protocols used to activate I_{Na} (delivered at 0.1 Hz), I_{Ba} (0.1 Hz), and macroscopic I_K (0.2 Hz).

plied to block $I_{K(A)}$. The remaining $I_{K(DR)}$, recorded in the presence of 4-AP, was then digitally subtracted from both controls and currents recorded in the presence of each κ-TRTX-Ec2 toxin. Although there was a small reduction in the amplitude of $I_{K(A)}$ in the presence of κ-TRTX-Ec2a, $I_{K(A)}$ at +30 mV was not significantly reduced by any of the κ-TRTX-Ec2 toxins ($p > 0.05$, two-way analysis of variance, $n = 3$; Fig. 5A). To assess whether κ-TRTX-Ec2 toxins alter the voltage-dependence of $I_{K(A)}$ channel activation, the current-voltage ($I_{K(A)}$-V) relationship in the presence of each toxin was determined using the same voltage protocol as for $I_{K(DR)}$-V curves. Again, in agreement with previous data from $I_{K(A)}$ recordings in DUM neurons, the threshold of $I_{K(A)}$ activation was at membrane potentials more depolarized than −50 mV (Grolleau and Lapied, 1995; Gunning et al., 2008). It is noteworthy that there were no significant shifts in the voltage-dependence of K_A channel activation for any κ-TRTX-Ec2 toxin ($\Delta V_{1/2} < 5.5$ mV for all toxins, $p > 0.05$, $n = 3$–7; Fig. 5B). In summary, the κ-TRTX-Ec2 toxins failed to inhibit $I_{K(A)}$ to an extent that could account for the 20 to 40% decrease seen in global K_V currents (Fig. 4C).

Like $I_{K(A)}$, BK_{Ca} channel currents [$I_{BK(Ca)}$] cannot be recorded in isolation from $I_{K(DR)}$ because, as mentioned previously, there are no selective blockers of insect $I_{K(DR)}$. Therefore, to isolate $I_{BK(Ca)}$, 5 mM 4-AP was included in external recording solutions. Both 30 nM ChTx and 1 mM $CdCl_2$ were also perfused at the conclusion of current recordings to eliminate $I_{BK(Ca)}$ allowing for offline subtraction of the remaining $I_{K(DR)}$. Although Cd^{2+} may modify many mammalian K_V channel currents, there is no evidence to suggest that this is the case in DUM neurons. Unfortunately, the use of ChTx, in the absence of Cd^{2+}, is insufficient to completely block BK_{Ca}

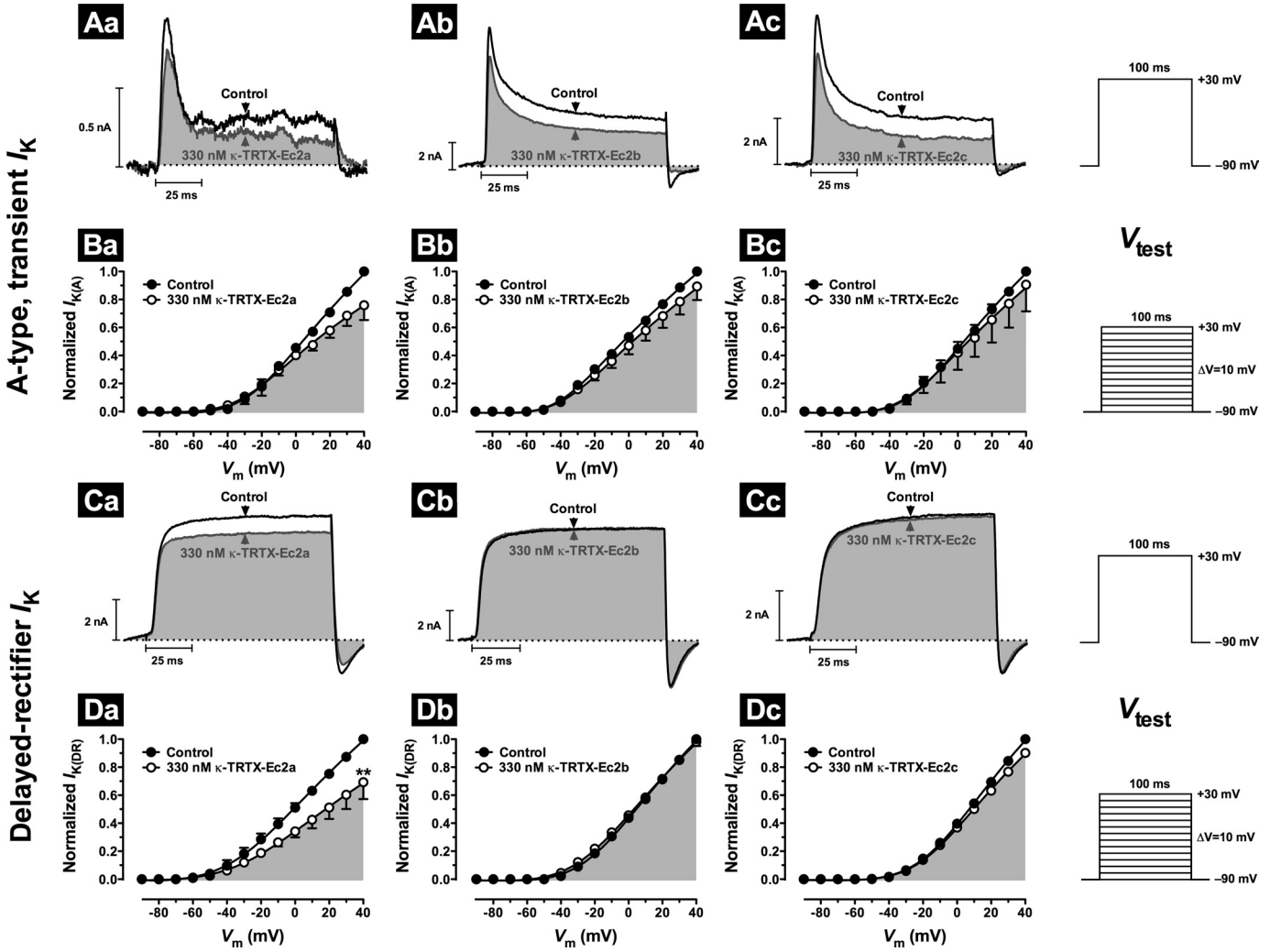

Fig. 5. Actions of κ-TRTX-Ec2 toxins on $I_{K(A)}$ and $I_{K(DR)}$ in cockroach DUM neurons. Panels show the effects of 330 nM κ-TRTX-Ec2a (a, left), 330 nM κ-TRTX-Ec2b (b, center), and 330 nM κ-TRTX-Ec2c (c, right), whereas the depolarizing voltage test pulse protocols used to elicit currents are shown at the far right. A and B, $I_{K(A)}$ were isolated in the presence of 30 nM ChTx and 1 mM $CdCl_2$, combined with current subtraction routines using 5 mM 4-AP (see *Results* for details). A, typical superimposed whole-cell $I_{K(A)}$ results were evoked by voltage steps to +30 mV from −90 mV for 100 ms in the presence, and absence, of toxin. B, families of whole-cell $I_{K(A)}$ were elicited by depolarizing test pulses from −90 to +40 mV in 10-mV increments. The membrane potential was then plotted against peak $I_{K(A)}$ amplitude and fitted to eq. 1. No significant shift in the threshold, or voltage midpoint, of activation of $I_{K(A)}$ was observed in the presence of 330 nM κ-TRTX-Ec2a (a, $n = 3$), κ-TRTX-Ec2b (b, $n = 7$), or κ-TRTX-Ec2c (c, $n = 3$). C and D, $I_{K(DR)}$ were isolated in the presence of 30 nM ChTx, 1 mM $CaCl_2$, and 5 mM 4-AP. C, typical superimposed whole-cell $I_{K(DR)}$ were evoked by voltage steps to +30 from −90 mV for 100 ms in the presence, and absence, of toxin. D, families of whole-cell $I_{K(A)}$ were elicited by depolarizing test pulses from −90 to +40 mV in 10-mV increments. The membrane potential was then plotted against late current amplitude measured at 100 ms and data fitted to eq. 1. No shift in the threshold, or voltage midpoint, of activation of $I_{K(DR)}$ occurred in the presence of 330 nM κ-TRTX-Ec2a (a, $n = 3$), κ-TRTX-Ec2b (a, $n = 3$), and κ-TRTX-Ec2c (a, $n = 7$). Data in B and D are expressed as the mean ± S.E.; **, $p < 0.01$.

channels, and previous studies of BK_{Ca} channel blockers in DUM neurons have all found it necessary to use Cd^{2+} to inhibit Ca^{2+} entry (Derst et al., 2003). In separate experiments, κ-TRTX-Ec2a, -Ec2b, or -Ec2c were then perfused for a period of 10 min, or until equilibrium was achieved. $CdCl_2$ (1 mM) and 30 nM ChTx were then applied to block BK_{Ca} channels. The remaining $I_{K(DR)}$, recorded in the presence of BK_{Ca} channel blockers, was then digitally subtracted from both control and currents recorded in the presence of each κ-TRTX-Ec2 toxin (Fig. 6B). All three toxins caused a similar

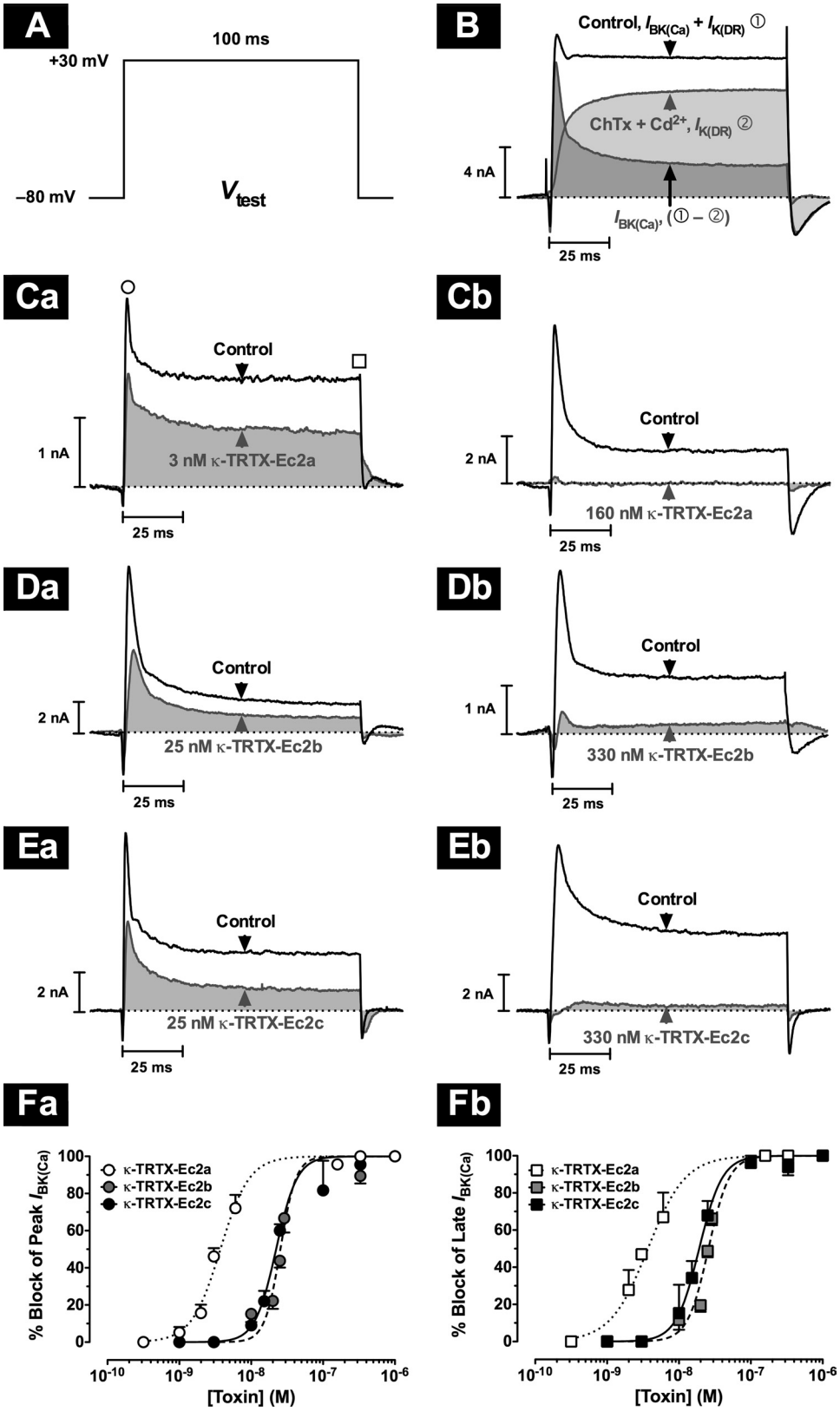

Fig. 6. κ-TRTX-Ec2 toxins block BK_{Ca} channel currents. A, whole-cell $I_{BK(Ca)}$ were recorded using the voltage test pulse protocol shown in A. Cells were held at −80 mV and stepped to +30 mV for a duration of 100 ms. B, current subtraction routine used to isolate BK_{Ca} channel currents (see *Materials and Methods*). C to E, typical effects of κ-TRTX-Ec2a, -Ec2b, and -Ec2c are shown in C, D, and E, respectively. Superimposed traces represent approximately 50% block of current (a) and close to complete block (b). F, concentration-response curves for inhibition of $I_{BK(Ca)}$ by κ-TRTX-Ec2 toxins measured from "fast-transient" $I_{BK(Ca)}$ (maximum peak outward current; circle in Ca) (Fa), and "late-sustained" $I_{BK(Ca)}$ (measured at 100 ms; square in Ca) (Fb). Data in F were fitted to eq. 2 and are expressed as the mean ± S.E. (n = 3–6).

concentration-dependent block of both transient and sustained $I_{BK(Ca)}$ at all concentrations tested. The IC_{50} values for block of $I_{BK(Ca)}$ by κ-TRTX-Ec2a, -Ec2b, and -Ec2c were 3.7, 25.3, and 24.6 nM for peak $I_{BK(Ca)}$ and 3.7, 25.8, and 19.1 nM for late $I_{BK(Ca)}$, respectively (Fig. 7, E and F). The approximately 6-fold higher potency of κ-TRTX-Ec2a versus Ec2b/Ec2c on peak and late $I_{BK(Ca)}$ maybe partially explained by the significant block of $I_{K(DR)}$ by κ-TRTX-Ec2a (Fig. 5, Ca and Da), which would cause an apparent increase in potency after $I_{K(DR)}$ subtraction routines in $I_{BK(Ca)}$ isolation procedures. Thus, although κ-TRTX-Ec2 toxins share considerable sequence homology with other spider toxins targeting Na_V, K_V, or Ca_V channels, some of which are promiscuous in their actions on multiple families of ion channel (e.g., β/ω-TRTX-Tp2a), the evidence from the present study indicates that κ-TRTX-Ec2 toxins act selectively on BK_{Ca} channels.

To assess whether κ-TRTX-Ec2 toxins block DUM neuron BK_{Ca} channels in a voltage-dependent manner, the $I_{BK(Ca)}$-V relationship in the presence of each toxin was determined. Families of $I_{BK(Ca)}$ were elicited by a series of 100-ms voltage pulses from a V_h of −80 to +40 mV in 10-mV increments at a frequency of 0.2 Hz. The threshold of $I_{BK(Ca)}$ activation was at membrane potentials greater than −40 mV, which is in agreement with previous data from BK_{Ca} channel recordings in DUM neurons (Grolleau and Lapied, 1995; Gunning et al., 2008). In the presence of 6 nM κ-TRTX-Ec2a, 25 nM κ-TRTX-Ec2b, or 25 nM κ-TRTX-Ec2c, there was no shift in the threshold or $V_{1/2}$ of $I_{BK(Ca)}$ activation of either peak or late $I_{BK(Ca)}$ (Fig. 7). Furthermore, channel block was not

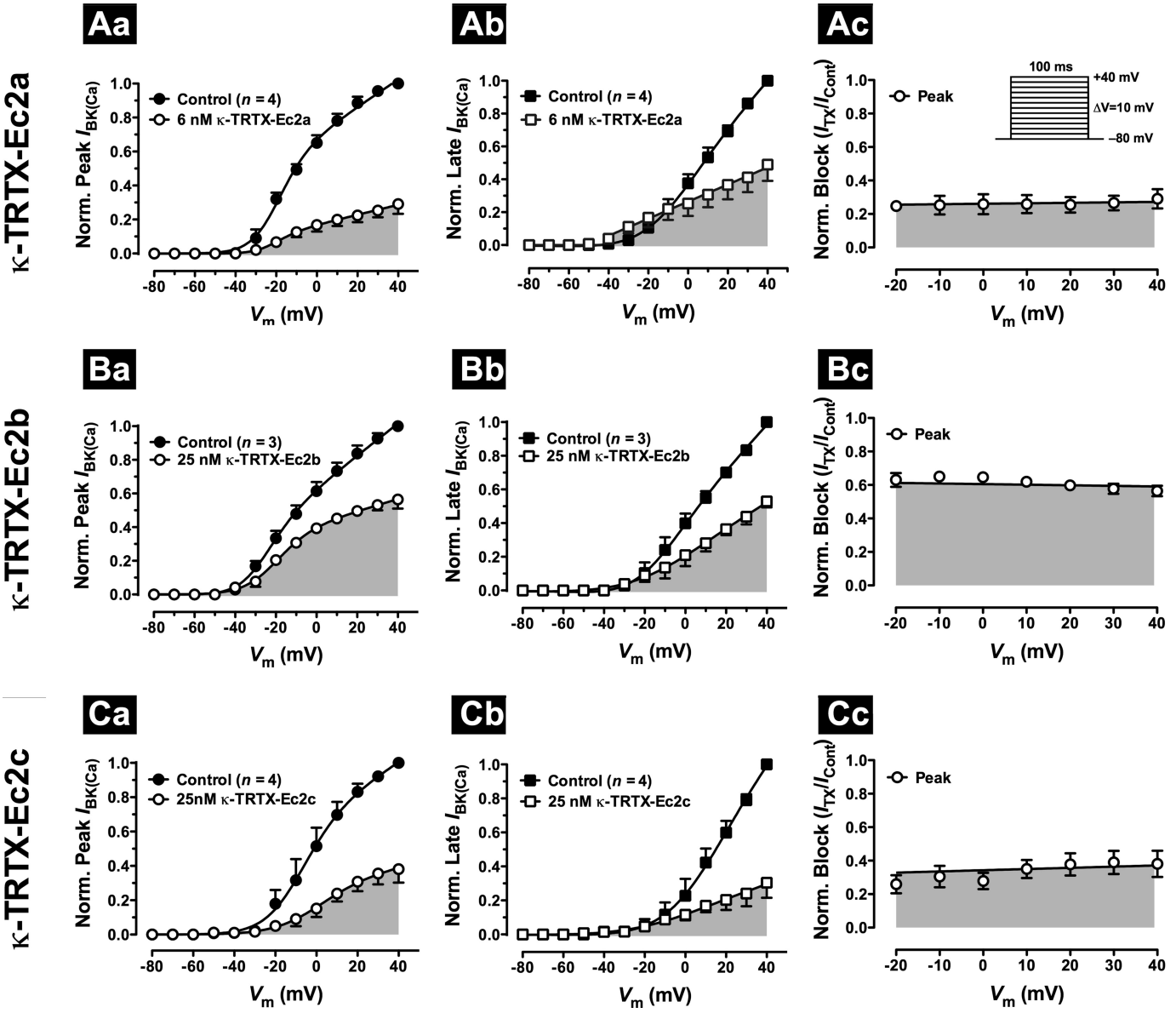

Fig. 7. Effects of κ-TRTX-Ec2 toxins on the voltage-dependence of BK_{Ca} channel activation in cockroach DUM neurons. Families of whole-cell $I_{BK(Ca)}$ were elicited by depolarizing voltage test pulses from −80 to +40 mV in 10-mV increments from a holding potential of −80 mV (see voltage test pulse protocol in Ac, inset). Whole-cell $I_{BK(Ca)}$-V relationships were recorded before (●) and after (○) perfusion with 6 nM κ-TRTX-Ec2a (A), 25 nM κ-TRTX-Ec2b (B), and 25 nM κ-TRTX-Ec2c (n = 3–4) (C). Measurements were taken from both fast-transient (a) and late-sustained $I_{BK(Ca)}$ (b) and fitted to eq. 1. No significant shifts in the voltage dependence of channel activation were observed. The right-hand column (c) shows the voltage dependence of the fractional block of fast-transient $I_{BK(Ca)}$ for κ-TRTX-Ec2 toxins (n = 3–4), taken from data in Aa to Ca. Data were expressed as the mean ± S.E. and fitted using linear regression.

relieved at increasing potentials (Fig. 7, Ac, Bc, and Cc), as noted for other voltage-dependent toxins, including many theraphosid spider toxins (Swartz, 2007).

Discussion

κ-TRTX-Ec2 Toxins Target Insect BK_{Ca}. Although all three of the κ-TRTX-Ec2 toxins share significant homology with a number of short-loop theraphotoxins acting on mammalian voltage-activated ion channels, they are unique from two perspectives. First, κ-TRTX-Ec2a and κ-TRTX-Ec2b are strictly insect-selective and thus show invertebrate phyla-selectivity not described previously for this group of toxins. Second, κ-TRTX-Ec2 toxins display high affinity and selectivity for the insect BK_{Ca} channel, a pharmacology previously only reported with κ-hexatoxin-Hv1c (Gunning et al., 2008), with whom they share no significant homology (Fig. 3B). As potent ligands for the insect BK_{Ca} channel, these toxins therefore represent valuable tools in the exploration of BK_{Ca} channel structure and characterizing the biological functions of insect BK_{Ca} channels. Indeed, these two families of toxins may become the defining pharmacology for insect BK_{Ca} channels.

Mode of Action. Several lines of evidence suggest that κ-TRTX-Ec2 toxins interact with their target via mechanisms unique from other theraphotoxins. Until the present study, K_V channel modulators from tarantula venoms were all characterized as gating-modifier toxins (Swartz, 2007). These toxins inhibit conductance by interfering with the voltage-sensing region of ion channels to cause a depolarizing shift in the voltage-dependence of activation thus stabilizing the closed or inactivated states of the channel. However, unlike all other theraphotoxins acting on K_V channels, BK_{Ca} current inhibition induced by the κ-TRTX-Ec2 toxins failed to exhibit any depolarizing shifts in the threshold, or voltage midpoint ($V_{1/2}$), of channel activation, clearly indicating that the mechanism of channel inhibition is not via the modulation of channel gating.

Other toxins interacting with K_V channels block ion conduction by physically occluding the pore of the channel near the selectivity filter. "Pore blockers" interact with amino acids situated in the S5–S6 linker and physically occlude the pore (Gross and MacKinnon, 1996). Among structurally dissimilar K_V channel pore blockers from sea anemone and scorpion venoms, a "functional dyad" is common to the bioactive surface of the molecules. This comprises an invariant lysine residue situated within 6.6 ± 1.0Å of an aromatic residue such as tyrosine or phenylalanine (Dauplais et al., 1997). This mode of action is similar to that reported for the insect-selective neurotoxin κ-HXTX-Hv1c, from the venom of the hexathelid spider *H. versuta*, that also inhibits BK_{Ca} channels (Gunning et al., 2008). Homology modeling of κ-TRTX-Ec2 toxins on the known structure of κ-TRTX-Gr2a (formerly GsMTx-2, Oswald et al., 2002; Protein Data Bank ID 1LUP), revealed several pairs of basic and aromatic residues that could satisfy the requirements of a functional dyad (Fig. 8). Possible functional dyads include Lys26-Trp24, Lys4-Phe5 (Lys5-Phe4 in κ-TRTX-Ec2c) and Lys14-Tyr1. However, none of these potential dyads are unique from residues in other β- or β/ω-TRTX toxins that do not target K_V channels (Fig. 3A). Moreover, there was no apparent voltage-dependence to the degree of block at various membrane potentials, with no reduction in block at higher potentials. Classic pore blockers such as charybdotoxin (α-KTx 1.1), κ-conotoxin PVIIA, and, to a lesser extent, κ-HXTX-Hv1c all demonstrate an alleviation of channel block at increasingly depolarized potentials as potassium driving force increases. As a consequence, these classic pore blockers all show moderate to strong voltage-dependent dissociation (Goldstein and Miller, 1993; Terlau et al., 1999; Gunning et al., 2008). Thus, the lack of voltage-dependent block by κ-TRTX-Ec2 toxins indicates that the toxins do not bind deeply into the extracellular mouth of the ion channel to plug the pore in a manner similar to other K_V and BK_{Ca} channel blockers.

Scorpion toxins that block small-conductance SK_{Ca} ($K_{Ca}2.x$) channels lack the conserved functional dyad present

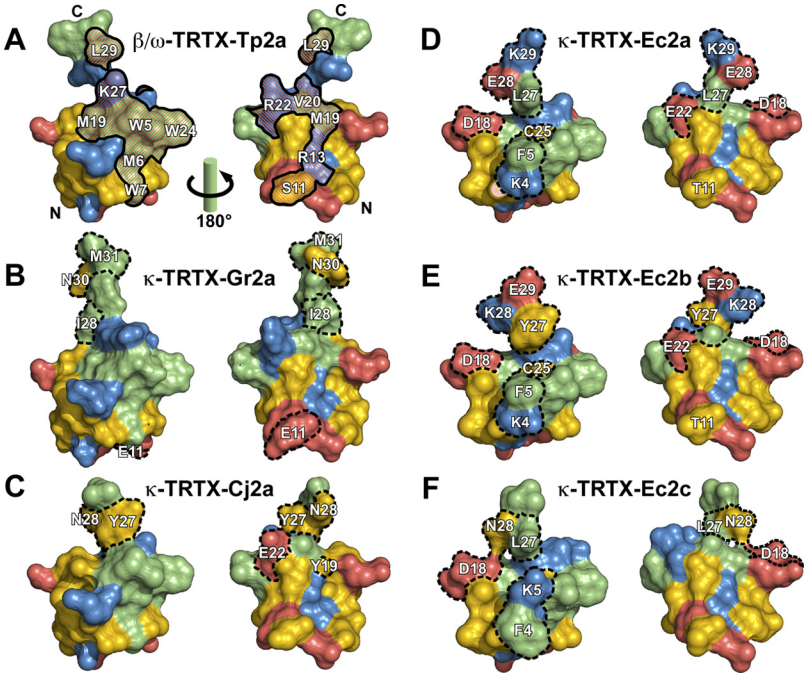

Fig. 8. Homology modeling of κ-TRTX-Ec2 toxins. All surface representations were modeled on the known NMR structure of the $K_V4.2/K_V4.3$-selective toxin κ-TRTX-Gr2a (B; Protein Data Bank ID 1LUP) using the automated protein homology-modeling server SWISS-MODEL. For each toxin, the right-hand structure has been rotated 180° about the *y*-axis. The colored regions on the surfaces represent basic, positively charged (blue), acidic, negatively charged (red), nonpolar, hydrophobic (green) and polar, noncharged (yellow) residues. A, surface representation of the Na_V- and $Ca_V1.3/Ca_V3.1$-selective β/ω-TRTX-Tp2a with the known pharmacophore residues for activity on $Na_V1.5$ channels highlighted (residues bounded by solid lines) (Smith et al., 2007). N and C termini are also shown. C to F, putative structures of the $K_V4.1$-selective κ-TRTX-Cj2a and the three BK_{Ca}-selective κ-TRTX-Ec2 toxins. Along with κ-TRTX-Gr2a, these structures depict key amino acids that are different from topologically equivalent residues in the pharmacophore of β/ω-TRTX-Tp2a (residues bounded by dotted lines). Surface representations were constructed using PyMOL version 1.3 for Macintosh.

in peptide pore blockers of K_V, IK_{Ca}, and BK_{Ca} channels. These toxins include, among others, scyllatoxin (α-KTx 5.1) and tamapin (α-KTx 5.4). Like κ-TRTX-Ec2 toxins, α-KTx 5.1 and α-KTx 5.4 have been shown to display a voltage-independent block of SK_{Ca} channels (Shakkottai et al., 2001; Pedarzani et al., 2002) and are believed to interact with the turret and loop region of the SK_{Ca} channel (Rodríguez de la Vega et al., 2003; Andreotti et al., 2005). Hence, these types of toxins are known as "turret blockers" to distinguish them from classic pore blockers. Unlike Lys27 within the functional dyad of α-KTx 1.1, which plugs the pore of K_V and BK_{Ca} channels and senses approximately 20% of the transmembrane electrical field (Goldstein and Miller, 1993), these SK_{Ca} toxins and κ-TRTX-Ec2 toxins all lack a Lys27 equivalent. Therefore, we predict that κ-TRTX-Ec2 toxins, like α-KTx 5 toxins, are likely to bind to the extracellular channel surface and act as turret blockers to completely inhibit ion flux. There exists the possibility that κ-TRTX-Ec2 toxins act to block the channel by acting as an electrostatic barrier rather than via steric occlusion of the channel. However, other toxins that cause such an electrostatic inhibition of channels do not completely inhibit current flow, resulting in a residual current (Hui et al., 2002). Given that κ-TRTX-Ec2 toxins can completely inhibit BK_{Ca} channel currents, we believe that they cause a direct steric occlusion of the channel.

Structure and Function. Although the key residues comprising the bioactive surface (pharmacophore) of κ-TRTX-Gr2a are currently unknown, the pharmacophore of the highly homologous β/ω-TRTX-Tp2a (formerly ProTx-II) for Na_V channels has been identified (Smith et al., 2007). Comparing the pharmacophore of the Na_V and Ca_V channel-selective β/ω-TRTX-Tp2a (Fig. 8A) and the surface of the K_V4-selective κ-TRTX-Gr2a and κ-TRTX-Cj2a (Fig. 8, B and C) with BK_{Ca}-selective κ-TRTX-Ec2 toxins, it can be seen that the major surface residues that differ for the κ-TRTX-Ec2 toxins are located at the C-terminal region (particularly residues 28–29), with additional mutations at positions 4 to 6, 11, 18, and 22 (Fig. 8, D–F). In particular, the presence of a glutamic acid residue at either position 28 or 29 in κ-TRTX-Ec2a and κ-TRTX-Ec2b is likely to confer insect-selectivity, because all of the remaining mammalian-active theraphotoxins have a basic or hydrophobic residue at one, or both, of these positions (Fig. 3A). Furthermore, affinity for the BK_{Ca} channel displayed by κ-TRTX-Ec2 toxins is likely to result from substitutions in the highly conserved Lys4-Trp5-Met6 of short-loop theraphotoxins (Fig. 3A), particularly because the apparent spatial location of Lys4-Phe5 of κ-TRTX-Ec2a and κ-TRTX-Ec2b (Phe4-Lys5 in κ-TRTX-Ec2c) is different from the other theraphotoxins (Fig. 8).

It is noteworthy that differences in the sequence of the K_V/BK_{Ca} channel target can also drastically alter the affinity of toxins for the channel complex. Although the selectivity filter and pore helix are well conserved across all potassium channels, the solvent-exposed turret and loop regions display high sequence variability and contribute to differences in α-KTx specificity (Giangiacomo et al., 2008). This can also extend to a variation in the size of the turret region. For example, the BK_{Ca} (Slo1) channel turret has six more residues with very limited sequence homology to the turret region of K_V1 channels (Giangiacomo et al., 2008). The size and sequence variability of the BK_{Ca} channel turret and loop regions could therefore explain the high selectivity of κ-TRTX-Ec2 toxins for BK_{Ca} over K_V channels. These sequence and size variations in the turret region also extend to subtle differences between the turret regions of various BK_{Ca} channels across different phyla. Although the size of the turret region of BK_{Ca} channels from vertebrates, marine invertebrates, and nematodes is believed to be the same, insect BK_{Ca} turret regions are typically one to three amino acids shorter (Giangiacomo et al., 2008; Gunning et al., 2008). Furthermore, single-point mutations in this region can result in dramatic changes in the phyletic selectivity of toxins (Myers and Stampe, 2000; Derst et al., 2003). Thus, the amino acid variation in the turret and loop regions of insect versus vertebrate BK_{Ca} channels seems to be sufficient to explain the insect selectivity of κ-TRTX-Ec2 toxins and κ-HXTX-Hv1c (Gunning et al., 2008).

It is noteworthy that subtle changes in toxin sequence can also drastically alter the affinity of the toxin for specific channel subtypes. For example, point mutations of Lys32 in α-KTx 1.1 result in mutants with markedly reduced affinity for $K_V1.2$ and $K_V1.3$ channels but little change in affinity for BK_{Ca} or IK_{Ca} channels (Rauer et al., 2000). In addition, a chimeric toxin construct involving residues from the α/β turn of iberiotoxin (α-KTx 1.3) grafted into noxiustoxin (α-KTx 2.1) causes a 50-fold weaker block of $K_V1.3$ channels but a >150-fold higher affinity for block of BK_{Ca} channels (Mullmann et al., 2001). These variations highlight that subtle differences in toxin sequence can have profound effects on channel subtype selectivity or specificity. This, together with variations in the amino acid sequence of channel subtypes, probably explains the different pharmacologies and modes of action of BK_{Ca}-selective κ-TRTX-Ec2 toxins versus other short-loop theraphosid spider toxins.

Novel Lead Compounds that Validate New Insecticide Targets. The κ-TRTX-Ec2 toxins represent the second family of toxins, along with κ-HXTX-Hv1c, to validate insect BK_{Ca} channels as potential targets for insecticides. As potent and selective blockers of insect BK_{Ca} channels, κ-TRTX-Ec2a and κ-TRTX-Ec2b toxins also represent valuable lead compounds in the development of future insect-selective biopesticides with a novel mode of action. Nevertheless, to undertake any structure-based rational insecticide design program, there is also a need to identify the residues responsible for phyla and target selectivity. Therefore, the close sequence homology between diverse short-loop theraphotoxins, displaying both phyla-selective neurotoxicity and diverse pharmacology, has afforded the unique opportunity to hypothesize on the molecular determinants for insecticidal and target selectivity. As a result, future mutagenesis experiments to determine the pharmacophore of the κ-TRTX-Ec2 toxins, guided by these hypotheses, should enable the determination of the residues responsible for insect selectivity and assist in the design of phyla-selective peptidomimetic insecticidal compounds.

Authorship Contributions

Participated in research design: Windley, Escoubas, Valenzuela, and Nicholson.

Conducted experiments: Windley, Escoubas, and Nicholson.

Performed data analysis: Windley, Escoubas, and Nicholson.

Wrote or contributed to the writing of the manuscript: Windley, Escoubas, Valenzuela, and Nicholson.

References

Andreotti N, di Luccio E, Sampieri F, De Waard M, and Sabatier JM (2005) Molecular modeling and docking simulations of scorpion toxins and related analogs on human SKCa2 and SKCa3 channels. *Peptides* **26:**1095–1108.

Chong Y, Hayes JL, Sollod B, Wen S, Wilson DT, Hains PG, Hodgson WC, Broady KW, King GF, and Nicholson GM (2007) The ω-atracotoxins: selective blockers of insect M-LVA and HVA calcium channels. *Biochem Pharmacol* **74:**623–638.

Corzo G, Diego-García E, Clement H, Peigneur S, Odell G, Tytgat J, Possani LD, and Alagón A (2008) An insecticidal peptide from the theraposid *Brachypelma smithi* spider venom reveals common molecular features among spider species from different genera. *Peptides* **29:**1901–1908.

Dauplais M, Lecoq A, Song J, Cotton J, Jamin N, Gilquin B, Roumestand C, Vita C, de Medeiros CL, Rowan EG, et al. (1997) On the convergent evolution of animal toxins. Conservation of a diad of functional residues in potassium channel-blocking toxins with unrelated structures. *J Biol Chem* **272:**4302–4309.

Derst C, Messutat S, Walther C, Eckert M, Heinemann SH, and Wicher D (2003) The large conductance Ca^{2+}-activated potassium channel (pSlo) of the cockroach *Periplaneta americana*: structure, localization in neurons and electrophysiology. *Eur J Neurosci* **17:**1197–1212.

Diochot S, Drici MD, Moinier D, Fink M, and Lazdunski M (1999) Effects of phrixotoxins on the Kv4 family of potassium channels and implications for the role of I_{to1} in cardiac electrogenesis. *Br J Pharmacol* **126:**251–263.

Edgerton GB, Blumenthal KM, and Hanck DA (2007) Modification of gating kinetics in $Ca_V3.1$ by the tarantula toxin ProTxII. Biophysical Society 51st Annual Meeting; 2007 Mar 3–7; Bethesda, MD. 2865-Pos. Baltimore, MD.

Escoubas P (2006) Molecular diversification in spider venoms: a web of combinatorial peptide libraries. *Mol Divers* **10:**545–554.

Escoubas P and Rash L (2004) Tarantulas: eight-legged pharmacists and combinatorial chemists. *Toxicon* **43:**555–574.

Escoubas P, Sollod B, and King GF (2006) Venom landscapes: mining the complexity of spider venoms via a combined cDNA and mass spectrometric approach. *Toxicon* **47:**650–663.

Giangiacomo KM, Becker J, Garsky C, Schmalhofer W, Garcia ML, and Mullmann TJ (2008) Novel α-KTx sites in the BK channel and comparative sequence analysis reveal distinguishing features of the BK and KV channel outer pore. *Cell Biochem Biophys* **52:**47–58.

Goldstein SA and Miller C (1993) Mechanism of charybdotoxin block of a voltage-gated K^+ channel. *Biophys J* **65:**1613–1619.

Grolleau F and Lapied B (1995) Separation and identification of multiple potassium currents regulating the pacemaker activity of insect neurosecretory cells (DUM neurons). *J Neurophysiol* **73:**160–171.

Gross A and MacKinnon R (1996) Agitoxin footprinting the shaker potassium channel pore. *Neuron* **16:**399–406.

Gunning SJ, Maggio F, Windley MJ, Valenzuela SM, King GF, and Nicholson GM (2008) The Janus-faced atracotoxins are specific blockers of invertebrate K_{Ca} channels. *FEBS J* **275:**4045–4059.

Herzig V, Wood DL, Newell F, Chaumeil PA, Kaas Q, Binford GJ, Nicholson GM, Gorse D, and King GF (2011) ArachnoServer 2.0, an updated online resource for spider toxin sequences and structures. *Nucleic Acids Res* **39 (Suppl 1):**D653–D657.

Hui K, Lipkind G, Fozzard HA, and French RJ (2002) Electrostatic and steric contributions to block of the skeletal muscle sodium channel by μ-conotoxin. *J Gen Physiol* **119:**45–54.

King GF (2007) Modulation of insect Ca_V channels by peptidic spider toxins. *Toxicon* **49:**513–530.

King GF, Escoubas P, and Nicholson GM (2008a) Peptide toxins that selectively target insect Na_V and Ca_V channels. *Channels* **2:**100–116.

King GF, Gentz MC, Escoubas P, and Nicholson GM (2008b) A rational nomenclature for naming peptide toxins from spiders and other venomous animals. *Toxicon* **52:**264–276.

Li D, Xiao Y, Hu W, Xie J, Bosmans F, Tytgat J, and Liang S (2003) Function and solution structure of hainantoxin-I, a novel insect sodium channel inhibitor from the Chinese bird spider *Selenocosmia hainana*. *FEBS Lett* **555:**616–622.

Maggio F and King GF (2002) Scanning mutagenesis of a Janus-faced atracotoxin reveals a bipartite surface patch that is essential for neurotoxic function. *J Biol Chem* **277:**22806–22813.

Middleton RE, Warren VA, Kraus RL, Hwang JC, Liu CJ, Dai G, Brochu RM, Kohler MG, Gao YD, Garsky VM, et al. (2002) Two tarantula peptides inhibit activation of multiple sodium channels. *Biochemistry* **41:**14734–14747.

Mullmann TJ, Spence KT, Schroeder NE, Fremont V, Christian EP, and Giangiacomo KM (2001) Insights into α-K toxin specificity for K^+ channels revealed through mutations in noxiustoxin. *Biochemistry* **40:**10987–10997.

Myers MP and Stampe P (2000) A point mutation in the maxi-K clone dSlo forms a high affinity site for charybdotoxin. *Neuropharmacology* **39:**11–20.

Nicholson GM (2007a) Fighting the global pest problem: preface to the special Toxicon issue on insecticidal toxins and their potential for insect pest control. *Toxicon* **49:**413–422.

Nicholson GM (2007b) Insect-selective spider toxins targeting voltage-gated sodium channels. *Toxicon* **49:**490–512.

Oswald RE, Suchyna TM, McFeeters R, Gottlieb P, and Sachs F (2002) Solution structure of peptide toxins that block mechanosensitive ion channels. *J Biol Chem* **277:**34443–34450.

Pallaghy PK, Nielsen KJ, Craik DJ, and Norton RS (1994) A common structural motif incorporating a cystine knot and a triple-stranded β-sheet in toxic and inhibitory polypeptides. *Protein Sci* **3:**1833–1839.

Pedarzani P, D'hoedt D, Doorty KB, Wadsworth JD, Joseph JS, Jeyaseelan K, Kini RM, Gadre SV, Sapatnekar SM, Stocker M, et al. (2002) Tamapin, a venom peptide from the Indian red scorpion (*Mesobuthus tamulus*) that targets small conductance Ca^{2+}-activated K^+ channels and afterhyperpolarization currents in central neurons. *J Biol Chem* **277:**46101–46109.

Rauer H, Lanigan MD, Pennington MW, Aiyar J, Ghanshani S, Cahalan MD, Norton RS, and Chandy KG (2000) Structure-guided transformation of charybdotoxin yields an analog that selectively targets Ca^{2+}-activated over voltage-gated K^+ channels. *J Biol Chem* **275:**1201–1208.

Rodríguez de la Vega RC, Merino E, Becerril B, and Possani LD (2003) Novel interactions between K^+ channels and scorpion toxins. *Trends Pharmacol Sci* **24:**222–227.

Salkoff L, Baker K, Butler A, Covarrubias M, Pak MD, and Wei A (1992) An essential 'set' of K^+ channels conserved in flies, mice and humans. *Trends Neurosci* **15:**161–166.

Shakkottai VG, Regaya I, Wulff H, Fajloun Z, Tomita H, Fathallah M, Cahalan MD, Gargus JJ, Sabatier JM, and Chandy KG (2001) Design and characterization of a highly selective peptide inhibitor of the small conductance calcium-activated K^+ channel, SkCa2. *J Biol Chem* **276:**43145–43151.

Smith JJ, Cummins TR, Alphy S, and Blumenthal KM (2007) Molecular interactions of the gating modifier toxin ProTx-II with NaV 1.5: implied existence of a novel toxin binding site coupled to activation. *J Biol Chem* **282:**12687–12697.

Swartz KJ (2007) Tarantula toxins interacting with voltage sensors in potassium channels. *Toxicon* **49:**213–230.

Terlau H, Boccaccio A, Olivera BM, and Conti F (1999) The block of Shaker K^+ channels by κ-conotoxin PVIIA is state dependent. *J Gen Physiol* **114:**125–140.

Wei A, Covarrubias M, Butler A, Baker K, Pak M, and Salkoff L (1990) K^+ current diversity is produced by an extended gene family conserved in Drosophila and mouse. *Science* **248:**599–603.

Wicher D and Penzlin H (1997) Ca^{2+} currents in central insect neurons: electrophysiological and pharmacological properties. *J Neurophysiol* **77:**186–199.

Address correspondence to: Dr. G. M. Nicholson, School of Medical and Molecular Biosciences, University of Technology, Sydney, P.O. Box 123, Broadway NSW 2007, Australia. E-mail: graham.nicholson@uts.edu.au